

# Mapping rice yield based on assimilation of ASAR data with rice growth model

YANG Shen-bin<sup>1</sup>, SHEN Shuang-he<sup>1</sup>, LI Bing-bai<sup>2</sup>, TAN Bing-xiang<sup>3</sup>, LI Zeng-yuan<sup>3</sup>

1. College of Applied Meteorology, Nanjing University of Information Science and Technology, Jiangsu Nanjing 210044, China;

2. Institute of Agricultural Resources and Environment, Jiangsu Academy of Agricultural Sciences, Jiangsu Nanjing 210014, China;

3. Institute of Forest Resources Information Technique, Chinese Academy of Forestry, Beijing 100091, China

**Abstract:** In this paper, a practical scheme for assimilation of multi-temporal and multi-polarization ENVISAT ASAR data in rice crop model to map rice yield is presented. To achieve this, rice distribution information is obtained first by rice mapping method to retrieve rice fields from ASAR images, and then an assimilation method is applied to use the temporal single-polarized rice backscattering coefficients which are grouped for each rice pixel to re-initialize ORYZA2000. The assimilation method consists of re-initializing the model with optimal input parameters allows a better temporal agreement between the rice backscattering coefficients retrieved from ASAR data and the ones simulated by a coupled model, i. e. , the combination of ORYZA2000 and a semi-empirical rice backscatter model through LAI. The SCE-UA optimization algorithm is employed to determine the optimal set of input parameters. After the re-initialization, rice yield for each rice pixel is calculated, and the yield map over the area of interest is finally produced. The scheme is applied over Xinghua study area located in the middle of Jiangsu Province of China during the 2006 rice season. The result shows that the obtained rice yield map generally overestimates the actual rice production by 13% , with a relative error of 11.2% at validation sites, but the tendency of rice growth status and spatial variation of the rice yield are well predicted and highly consistent with the actual production variation.

**Key words:** assimilation strategy, remote sensing, ASAR, rice yield prediction, crop model

**CLC number:** TP79 **Document code:** A

## 1 INTRODUCTION

Rice is a staple food crop in China and its annual yield accounts for half of the country's total crop production (Yu *et al.*, 1980), showing its importance in keeping China's fast development. Since remote sensing technique has improved in decades, quick and continuous monitoring of agricultural crops can be done through satellites. However, more than 90% of rice is planted in southern China where always retains plentiful rainfall and dense cloud cover during the rice season (Yu *et al.*, 1980). Therefore, rice crop monitoring entails the use of microwave remote sensing, since microwave can penetrate through clouds and has all-weather capabilities.

Since the launch of ENVISAT satellite which carries a powerful Advanced Synthetic Aperture Radar (ASAR), a large amount of radar data have been obtained to serve both scientific and application-oriented users. ASAR operates at C-band frequency of 5.3 GHz and can provide radar product in five working modes, among

which Alternative Polarization Mode (APMode) contains two simultaneous images from the same area in HH and VV polarizations, HH and HV, or VV and VH, with the same imaging geometry. In crop monitoring, the effectivity and reliability of ASAR APMode product have been confirmed by many researches (Dente *et al.*, 2007; Mattia *et al.*, 2003; Stankiewics, 2006). For rice, most of the reports are focused on rice mapping (Chen *et al.*, 2007; Tan *et al.*, 2006; Yang *et al.*, 2008a), rice parameters retrieval (Yang *et al.*, 2008a) and rice backscattering mechanism (Dong *et al.*, 2006). However, the potential of ASAR data in rice yield estimation has not been fully investigated.

During the last decade, methods of integrating remote sensing data into crop models for crop production forecast have been widely used and promoted, which not only solved the technical issue in parameterization for regional crop models application, but also improved the accuracy of regional crop yield estimation (Moulin *et al.*, 1998; Zhao *et al.*, 2005). There are two main methods: one is the 'driving' method; the other is the assimilation method. The assimilation method is used to

**Received date:** 2008-01-25; **Accepted date:** 2008-03-30

**Foundation:** Jiangsu Graduate in Scientific Research and Innovation (No. CX07B\_048z), and the Special Program for Scientific Research in Public Welfare Meteorological Services (No. GYHY200806008).

**First author biography:** YANG Shen-bin (1981— ), male, Ph. D in agricultural remote sensing, and a lecturer of Nanjing University of Information Science & Technology, has published 6 papers.

optimize a crop model by minimizing the difference between the radiometric signal and its simulation by the re-parameterization and/or re-initialization of the crop production model. Ma *et al.* ( 2005 ) showed the accuracy was improved by applying this method to simulate the growth status of winter wheat in the east of China. Yan *et al.* ( 2006 ) adopted this method to assess the influence of different assimilation data source to the simulation results.

In this paper, a practical scheme for mapping rice yield based on multi-temporal and multi-polarization ASAR data is presented, in which the assimilation method has been adopted, and validated using the data acquired in 2006 over the Xinghua study area located in the middle of Jiangsu Province of China.

2 EXPERIMENTS AND DATA

2.1 Study Area and Experiments

The study area is an agricultural area of 90 km<sup>2</sup> located in the middle of Jiangsu Province of China, approximately 32° 51' N—32° 58' N and 120° 00' E—120°06' E. The landscape is flat with intensive water network and fertile soil belonging to the Lixiahe grain-producing area of Jiangsu Province. The crop system here is a two-crop rotation system, with wheat in winter and rice in summer. During the rice season, more than 95% of rice is direct-seeded. The dominant rice species is japonica rice with a life span of about 135 days. Other crops include bean, cotton, corn and vegetables.

In 2006, four rice growth monitoring plots A, B, C and D with size of about 10 ha each were established, and ground truth data were collected from the plots at 10-day interval from June 25<sup>th</sup> to October 20<sup>th</sup>. The distance between each two plots ranges from 0.3 km to 3 km. Within each plot, 5 fixed observation sites with area of 1 m<sup>2</sup> each were monitored for rice growth stages, plant density, plant height and general information about field management. The above ground biomass were measured separately for stems, ears green and dead leaves, by collecting 25 samples randomly within each plot and weighing them before and after drying at 80°C for 48 h.

LAI was measured by a direct method. During the rice harvest, detailed information on actual rice production was collected within the study area for validation. Meanwhile, boundaries of the monitoring plots and other land surface objects were recorded using DGPS devices. Soil surface profile of 1 m length was also measured in both vertical and horizontal directions. In addition, daily meteorological data were obtained from local meteorological bureau, including maximum and minimum temperature, vapor pressure, mean wind speed, rainfall and sunshine duration. Table 1 provides the basic information on average rice growth conditions of each monitoring plot.

Table 1 Information on average rice growth condition

Plot	Plant density ( plant/m <sup>2</sup> )	Date of rice seeding	Date of rice heading	Final yield ( kg/ha )
A	215	June 10, 2006	August 28, 2006	9370
B	294	June 11, 2006	August 29, 2006	10380
C	233	June 11, 2006	September 1, 2006	9379
D	240	June 12, 2006	September 1, 2006	9068

2.2 ASAR Data

During the rice season of 2006, four ASAR APMODE products were acquired over the study area ( Table 2 ). The calibration was carried out using the BEST software provided by European Space Agency ( ESA ) to extract backscattering coefficients. In order to reduce the speckle noise, two SAR image filters, the multi-channel filter ( Quegan and Yu, 2001 ; Yang *et al.*, 2006 ) and GAMMA MAP filter ( Kuan *et al.*, 1987 ), were performed successively to the previously calibrated images. With the data set, the resulting filtered images reached an ENL ( i. e. equivalent number of look ) of 64. Images were geo-referenced in ENVI software using a scene of geo-corrected ETM image with a root mean square error of the control points of about 22 m.

Finally, backscattering coefficients of different crops and other land surface objects were extracted and spatially averaged over the obtained sample files for HH and VV polarizations respectively.

Table 2 Overview of the acquired ASAR data and the phenological stage of rice at each of the acquisition date

Acquisition	Polarization	Orbit	Spatial resolution	Incidence angle	Rice phenological stage
06/30/2006	HH/VV	Descending	30 m	19.2°—26.7°	Tillering stage
08/04/2006	HH/VV	Descending	30 m	19.2°—26.7°	Jointing stage
08/19/2006	HH/VV	Ascending	30 m	19.2°—26.7°	Booting stage
09/23/2006	HH/VV	Ascending	30 m	19.2°—26.7°	Grain filling stage

3 SCHEME FOR MAPPING RICE YIELD BASED ON ASAR DATA

Shao *et al.* (2001) put forward a scenario for rice yield estimation based on multi-temporal radar data. The plot requires many supporting data, such as DEM, soil map, crop data; and techniques, such as GIS, image classification and rice modeling that complicates the implementation of the whole scheme for practical purpose. Therefore, this paper presents a simplified and practical rice yield mapping scheme based on ASAR data (Fig. 1). It consists of two parts for realizing the whole process. In the first part, ASAR data is combined with rice mapping method to obtain the rice distribution map over the area of interest. The rice map is used to mask all the ASAR images to select only rice fields and retrieve rice backscattering coefficients. It should be noted that the accuracy of rice yield estimation is somehow influenced by the rice mapping accuracy. Therefore, multi-temporal and multi-polarization radar data are recommended for rice mapping, because rice mapping accuracy higher than 80% has been reported in several studies with the threshold of supervised classification method (Yang *et al.*,

2008a, 2008b; Zhang *et al.*, 2006). The second part in this scheme is mainly shown in the dashed box in Fig. 1, where an assimilation method is adopted to calculate the rice yield for each rice pixel. The assimilation method is the direct use of observed rice backscattering coefficients to re-initialize the rice growth model ORYZA2000. ORYZA2000 is coupled with a semi-empirical rice backscatter model using LAI as an essential link to simulate rice backscattering coefficients. The assimilation method re-initializes the ORYZA2000 model with optimal input parameters allowing a better temporal agreement between the rice backscattering coefficients simulated and those observed. The global optimization algorithm SCE-UA is applied to determine the optimal set of input parameters. After the re-initialization, rice yield corresponding to each rice pixel is calculated by ORYZA2000, and finally, the rice yield map of the area of interest is produced.

The rice map of the study area was retrieved from our previous study (Yang *et al.*, 2008a) with mapping accuracy of 84.36%, which indicates that the rice map can be employed in this study directly. Therefore, only models and optimization algorithm are described in details in the next part.

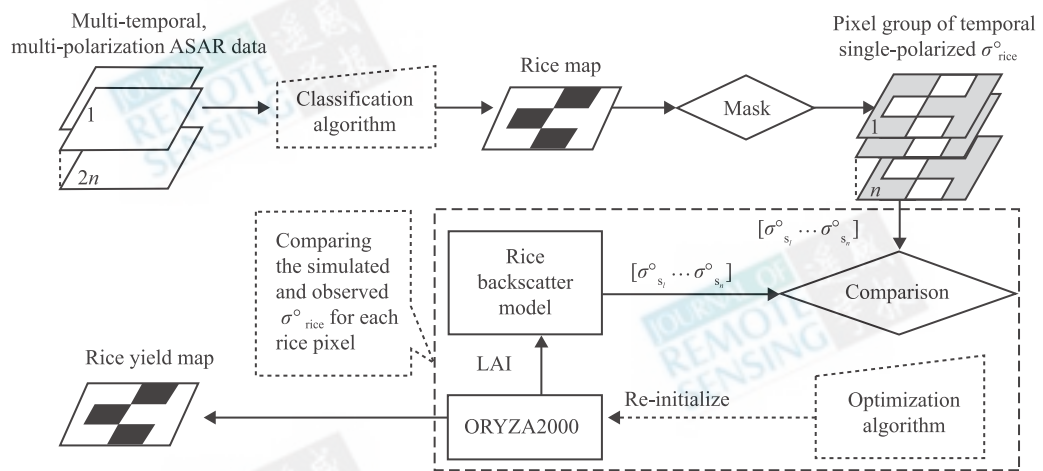


Fig. 1 Scheme for mapping rice yield based on ASAR data

4 MODELS AND ALGORITHM

4.1 ORYZA2000

ORYZA2000 is a dynamic, eco-physiological rice crop model to simulate the growth, development and water balance of lowland rice in situations of potential production, water limitations and nitrogen limitations (Bouman *et al.*, 2001; Xue *et al.*, 2005). To simulate all these production situations, several modules are combined, such as modules for aboveground crop

growth, evapo-transpiration, nitrogen dynamics, and soil-water balance, in which large number of model parameters and specific *in-situ data* (i. e. weather data, field management data and soil data) are required to run the model successfully. A large number of parameters are contained in ORYZA2000, but most of them are universal (i. e. not sensitive to rice species); only parameters accounting for rice development, biomass distribution and photosynthetic ratio need to be calibrated corresponding to different rice species.

In this study, rice growth is assumed in the situation of potential production, for which rice grows with ample



supply of water and nutrients and the growth rates are determined by rice physiological characteristics and weather conditions. In order to obtain accurate predictions for the growth of japonica rice under consideration, the calibration of ORYZA2000 should be carried out to estimate the variety-specific parameters which consist of development rate, partitioning factors, relative leaf growth rate, specific leaf area, leaf death rate and fraction of stem reserves. Two programs DRATES and PARAM provided by ORYZA2000 are performed for the calibration using the experimental data collected over the plots A and B. The experimental data of the plots C and D are kept for the validation. After the calibration, the result showed that the average difference between the simulated and observed rice development stages was less than one day, and the final yield was predicted with a simulation error less than 18%. The correlation coefficient of simulated and measured LAI reaches 96%. Taking into account the uncertainties of calibration process caused by the ground measurement errors, the calibration results can be considered acceptable in the context of a crop growth model.

Even though the genotype parameters are identified during the calibration procedure, the ORYZA2000 model still needs a large number of input parameters. Among them, some parameters can vary greatly over the study area and are rarely available through field measurements. Therefore, a sensitivity analysis is carried out to determine whether or not there exists a relatively small subset of model inputs affecting, more than others, the temporal behavior of the state variables of interest for the assimilation. The result shows that the predicted rice yield and LAI are mainly sensitive to the changes of emergence date (EMD) and plant density (NPLDS). While the emergence date delays or advances for 10 days, the simulated flowering date would vary 8–10 days and the average variation in simulated rice yield reach 5.3% and 4.8% for simulated maximum LAI. Since rice is direct-seeded, the difference between plant densities from fields to fields reaches more than 22% on average and 69% to the maximum, showing that the plant density varies remarkably over the study area. It shows that while the plant density increases 100 plant/m<sup>2</sup>, there would be an average change of 4.6% in simulated rice yield and 10% in simulated maximum LAI. Therefore, rice emergence date and plant density constitute the set of model inputs which are involved in the assimilation and re-initialization process.

## 4.2 Cloud

Attema and Ulaby (1978) presented a semi-empirical

radar model to simulate the volume scattering for vegetation. It assumes that vegetation consists of a collection of water droplets, which are represented as small identical particles, if the volume scattering is the predominant mechanism responsible for the backscatter from canopy. The simple model can be expressed as the first order solution of the radiative transfer equations (1)–(3) to compute the backscattering coefficient  $\sigma^\circ$  for the vegetation:

$$\sigma^\circ = \sigma_{\text{veg}}^\circ + k^2 \cdot \sigma_{\text{soil}}^\circ \quad (1)$$

$$\sigma_{\text{veg}}^\circ = \alpha \cdot \cos\theta \cdot (1 - k^2) \quad (2)$$

$$k^2 = \exp(-2 \cdot \beta \cdot W \cdot h / \cos\theta) \quad (3)$$

where  $\sigma_{\text{veg}}^\circ$  = backscattering coefficient for vegetation canopy/ (m<sup>2</sup>/m<sup>2</sup>)

$\sigma_{\text{soil}}^\circ$  = backscattering coefficient for soil/ (m<sup>2</sup>/m<sup>2</sup>)

$k^2$  = two-way attenuation through the canopy

$\alpha$  = backscattering coefficient at full closure of the canopy/ (m<sup>2</sup>/m<sup>2</sup>)

$\beta$  = coefficient of attenuation per unit of canopy water/ (m<sup>2</sup>/kg)

$\theta$  = incident angle of radar beam/(°)

$W$  = amount of canopy water unit volume/ (kg/m<sup>3</sup>)

$h$  = canopy height/m

The simple model was applied successfully for a range of crop types (*e. g.* winter wheat, bean) and conditions (Wigneron *et al.*, 1999; Bouman *et al.*, 1999; Graham & Harris, 2002). For paddy rice, we simply assume the scattering from the paddy background (water surface) is constant before the ripening stage and the temporal variation of rice backscatter is mainly attributed to the change of canopy size (*e. g.*, stem height, leaf size), canopy water content and canopy biomass. The same assumption was also made by Inoue *et al.* (2002) to analyze the interaction between rice backscattering coefficients and plant variables.

In order to link the simple model with ORYZA2000 by the LAI, regression analysis is applied to investigate the relationship between  $W \cdot h$  and LAI, in which the  $W \cdot h$  represents the canopy water content per unit soil surface (kg/m<sup>2</sup>). As a result, a significant relationship is found as the following rational equation:

$$\text{LAI} = \frac{a \cdot W \cdot h + b}{W \cdot h + c} \quad (4)$$

where  $a$ ,  $b$  and  $c$  are coefficients equalling 0.19, 0.1534 and 1.511 respectively.

Fig. 2 shows the obtained best fit curve with goodness-of-fit statistics. The high fitting level implies that the LAI can be substituted for the  $W \cdot h$  in the simple model to simulate rice backscatter. Finally, the Cloud model for the rice paddy can be expressed (in dB) as follows:

$$\sigma^{\circ} = 10\log_{10} [\alpha \cdot \cos\theta \cdot (1 - k^2) + k^2 \cdot \sigma^{\circ}_{BG}] \quad (5)$$
$$k^2 = \exp \{ -2 \cdot \beta \cdot (b - c \cdot \text{LAI}) / [(\text{LAI} - a) \cdot \cos\theta] \} \quad (6)$$

where  $\sigma^{\circ}_{BG}$  = constant backscattering from canopy background/(m<sup>2</sup>/m<sup>2</sup>)

Here, three parameters  $\alpha$ ,  $\beta$  and  $\sigma^{\circ}_{BG}$  should be estimated by fitting the model to the observed rice backscatter data. In this paper, the global optimization method SCE-UA is applied to estimate the optimal values of the three parameters, and tested for HH and VV polarization separately. The brief description of SCE-UA method and optimization configurations can be found in the next part. Table 3 provides the results in terms of  $\alpha$  (in dB),  $\beta$  and  $\sigma^{\circ}_{BG}$  (in dB) with some statistics, which indicate the Cloud model calibrated in HH polarization has a better performance in simulating the rice backscattering coefficients.

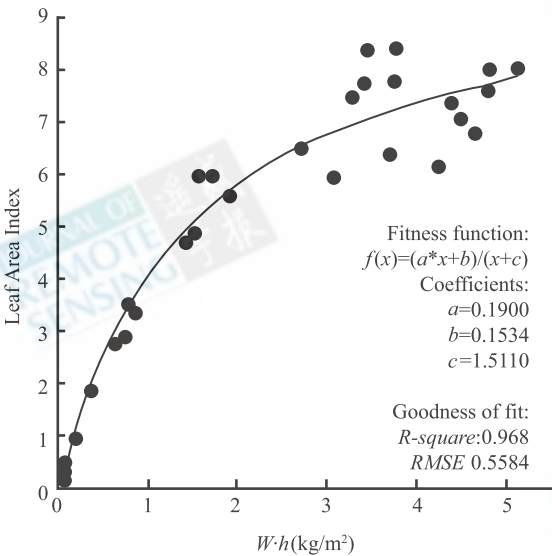


Fig. 2 Regression and curve fitting analysis between  $W \cdot h$  and LAI with statistical results

Table 3 Optimal values of parameter  $\alpha$ ,  $\beta$  and  $\sigma^{\circ}_{BG}$  with statistical results for HH and VV respectively

Polarization	$\alpha$ /dB	$\beta$ /m <sup>2</sup> /kg	$\sigma^{\circ}_{BG}$ /dB	Plot	R	RMSE
HH	- 5.2982	5.8091	- 118.4061	A	0.9775	0.8733
				B	0.9576	1.1560
				C	0.9658	1.0448
				D	0.9923	0.7229
VV	- 150.7583	0.0444	- 7.9250	A	0.4071	1.0531
				B	- 0.9314	0.9925
				C	0.8664	0.7886
				D	0.9894	1.0551

4.3 SCE-UA Algorithm

The global optimization algorithm SCE-UA (Shuffled Complex Evolution) is developed by Duan in 1993 (Duan *et al.*, 1993). It is not problem specific and is easy to handle, which has been widely used in various fields for nonlinear optimization problems and reported exact results (Duan *et al.*, 1994; Li *et al.*, 2004). The SCE-UA algorithm contains many parameters that control the probabilistic and deterministic components of the method. Here, we only present the optimization configuration for the

model input parameters of the rice backscatter model and ORYZA2000, with the system settings of the SCE-UA method for each of them (see Table 4 and 5). Least-square function is used as the objective function. The optimization process is terminated if one of the following criteria is satisfied: (1) the algorithm is unable to improve 0.0001 percent for the value of the objective function over five iterations; (2) the algorithm is unable to change the parameter values and simultaneously improve the function value over five iterations; (3) the maximum number of iterations (10000) is exceeded.

Table 4 Initial values and sample intervals of model input parameters for rice radar model and coupled model

Configuration	Rice backscatter model			ORYZA2000	
	$\alpha$ /(m <sup>2</sup> /m <sup>2</sup> )	$\beta$ /(m <sup>2</sup> /kg)	$\sigma^{\circ}_{BG}$ /(m <sup>2</sup> /m <sup>2</sup> )	EMD/d	NPLDS/(plants/m <sup>2</sup> )
Initial value	0.143	8.2	0.083	166	230
Sample interval	(0, 1)	(0,10)	(0, 1)	[145, 175]	[100, 300]

Table 5 System settings of SCE-UA for rice radar model and coupled model

Models	Number of Complexes	Number of points in each complex	Number of points in a sub-complex	Number of evolution steps	Minimum number of complexes	Trials
Cloud	4	7	4	7	3	10
ORYZA2000	3	5	3	5	2	10

5 RESULTS

The assimilation was carried out for a total of 31388 pixels to calculate the regional rice yield. During the

process, the optimization stopped successfully in criteria (1), and recorded the optimal values of EMD and NPLDS for further analysis. In order to map the rice yield of the study area, the whole process costs about five days to complete using a desktop computer with CPU of 1.5GHz.

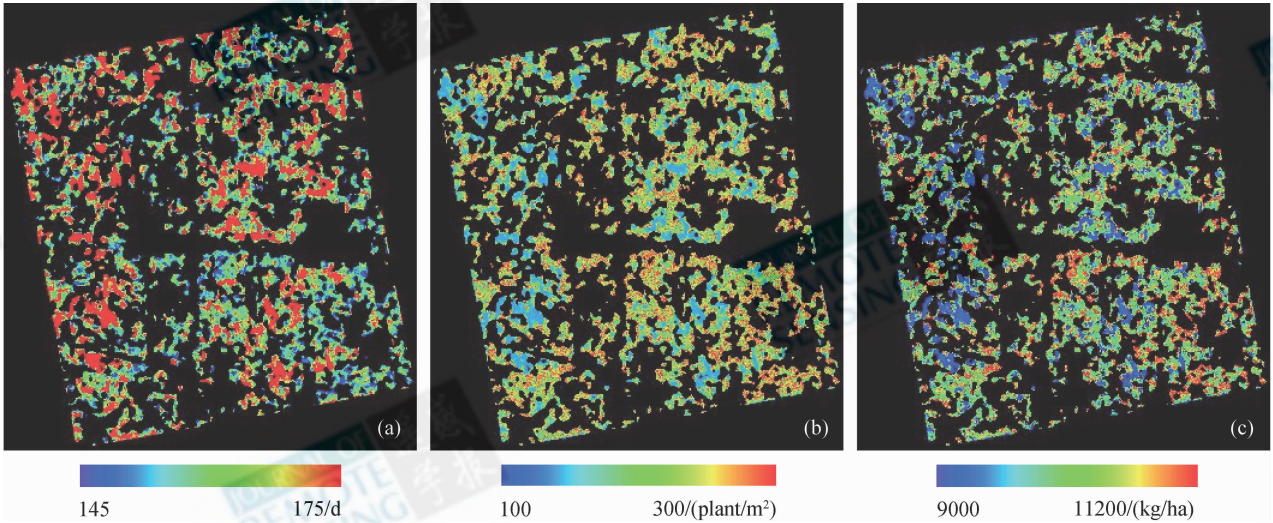


Fig. 3 Maps of (a) rice emergence date, (b) rice plant density and (c) final production

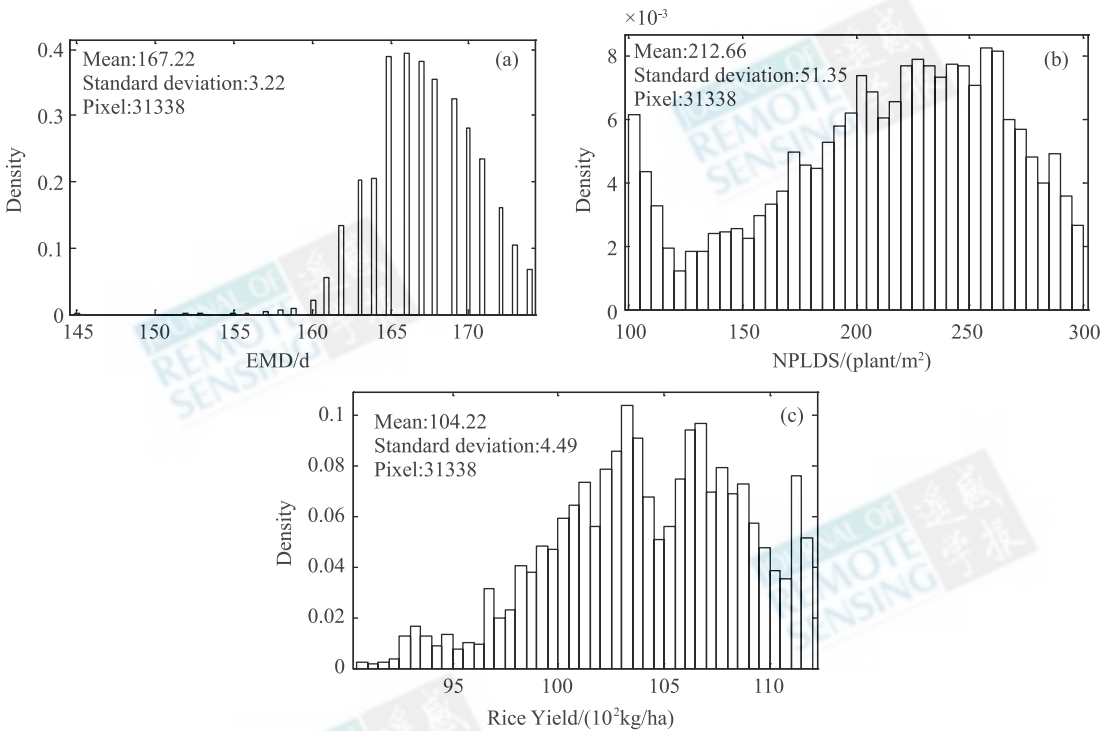


Fig. 4 Density of pixel values for maps of (a)rice emergence date, (b) rice plant density and (c) final production



Fig. 3 shows the obtained distribution maps of EMD and NPLDS and the estimated rice yield with spatial resolution of 30 m. For each map, different colors are assigned to the pixels according to their values. The probability density plots of the retrieved maps were also displayed in Fig. 4. It shows that the optimal parameters vary mainly in the following ranges: the EMD between 160d and 175d, and the NPLDS between 150 and 300 plant/m<sup>2</sup>. According to our field survey, the variation of the estimated EMD and NPLDS is realistic for the study area, except that the average NPLDS is slightly underestimated by 30 plant/m<sup>2</sup>. The rice yield in Fig. 3 (c) varies between 9000 and 11200 kg/ha. The mean estimated is about 10422 kg/ha, higher than the average observed about 1200 kg/ha (i.e. approximately 13%).

For a quantitative evaluation of the reliability of the produced rice yield map, it was compared to the *in-situ* data collected over the 10 monitored fields. As shown in Fig. 5, it was found that the estimated rice yield is generally higher than the observed with a root mean square error of approximately 1133 kg/ha and a relative error of 11.2%. A high difference of about 2000 kg/ha between the estimated and observed was found in the monitored field 6 and 7 where rice was grown under unfavorable conditions. The overestimation of the rice yield was due to the simulation under the condition of potential production used in this study.

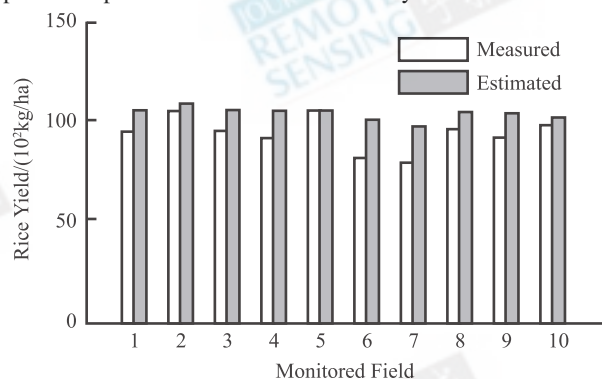


Fig. 5 Comparison between measured and simulated rice yield

In fact, although the condition of rice growth in the study area is favorable with abundant water and active field management, rice disease and pests (e.g. rice planthopper) are still severe during the rice growth period of 2006, which causes the universal reduction of the rice yield. However, the tendency of rice growth status and final yield are well predicted. According to the field survey during the rice harvest, the predicted spatial variation of the rice yield is highly consistent with the actual rice production situation.

## 6 CONCLUSION AND DISCUSSION

In this study, a practical scheme for mapping rice yield

based on multi-temporal and multi-polarization ASAR data is presented. It consists of two parts: one is rice mapping, and the other is rice yield estimation using assimilation method. The scheme is applied over Xinghua study area of China and validated with experimental data collected in 2006. Rice map was produced in a previous study by ASAR data. The mapping accuracy reached 84.36%. ORYZA2000 is calibrated using the field measurements to obtain the variety-specific parameters. The sensitivity analysis is carried out subsequently to identify the most suitable model inputs to be involved in the re-initialization, i.e. the parameters which mainly affect LAI and final yield predictions. The results shows that LAI and final yield are mainly sensitive to the rice emergence date and rice plant density. The semi-empirical rice backscatter model is calibrated to simulate the HH-polarized rice backscattering coefficients instead of the VV-polarized ones.

The ORYZA2000 model predicts a rice yield map with a spatial resolution of 30 m. The result shows that the obtained rice yield map generally overestimates the actual rice production by 13%, with a relative error of 11.2% on validation sites. This is due to the potential rice growth conditions assumed. But the tendency of rice growth status and final yield are well predicted and the spatial variation of the rice yield is highly consistent with the actual rice production situation.

In conclusion, the scheme described in this study is a promising technique to apply on multi-temporal and multi-polarization radar data and rice crop models for regional rice production estimation, when no accurate *in-situ* information is available and/or optical data are hampered by heavy clouds during the rice season. However, further validation of the presented scheme at different rice planting areas and with different radar configurations (e.g. incidence angle, polarization) is needed, with the suggestions to improve the effectiveness of the proposed scheme:

(1) Considering the influence of actual unfavorable conditions, like water limit, nutrient limit and insect pest to rice growth simulation.

(2) Improve the Cloud model for rice paddy, especially considering the contribution of water surface during early rice season to rice backscatter (Le Toan *et al.*, 1997; Koay *et al.*, 2007).

(3) Increase the optimization threshold of SCE-UA algorithm to 0.0001%, in order to avoid the insensitivity of the Cloud model to LAI.

**Acknowledgements** This work received great help from Prof. Thuy Le Toan of ESA, who is a foreign-expert leading the ESA-NRSCC Dragon Cooperation Program (<http://earth.esa.int/dragon/>). The authors are also grateful to ESA for supplying the ASAR images, and would like to thank Prof. B. A. M. Bouman of the International Rice Research Institute (IRRI) for

permitting us to use the ORYZ2000 model, and thank Dr. Q. Y. Duan of the Lawrence Livermore National Laboratory, for providing the program of the SCE-UA algorithm.

## REFERENCES

- Attema E P W and Ulaby F T. 1978. Vegetation modeled as a water cloud. *Radio Science*, **13**(2):357—364
- Bouman B A M, Van Kraalingen D W G, Stol W and Van Leeuwen H J C. 1999. An agroecological modeling approach to explain ERS SAR radar backscatter of agricultural crops. *Remote Sensing of Environment*, **67**:137—146
- Bouman B A M, Kropff M J, Tuong T P, Wopereis M C S, Berge H F M ten and Laar H H van. 2001. ORYZA2000: Modeling lowland rice. International Rice Research Institute, Los Baños, Philippines, and Wageningen University and Research Center, Wageningen, Netherlands
- Chen J S, Lin H and Pei Z Y. 2007. Application of ENVISAT ASAR data in mapping rice crop growth in southern China. *IEEE Geoscience and Remote Sensing Letters*, **4**(3):431—435
- Dente L, Satalino G, Mattia F and Michele R. 2008. Assimilation of leaf area index derived from ASAR and MERIS data into Ceres-Wheat model to map wheat yield. *Remote Sensing of Environment*, **112**(4): 1395—1407
- Dong Y F, Sun G Q and Pang Y. 2006. Monitoring of rice crop using ENVISAT ASAR data. *Science in China; Series D Earth Sciences*, **49**(7):755—763
- Duan, Q, Gupta V K and Sorooshian S. 1993. A shuffled complex evolution approach for effective and efficient global minimization. *Journal of Optimization Theory and Its Applications*, **61**(3):501—521
- Duan Q Y, Sorooshian S and Gupta V K. 1994. Optimal use of the SCE-UA global optimization method for calibrating watershed models. *Journal of Hydrology*, **158**:265—284
- Graham A J and Harris R. 2002. Estimating crop and waveband specific water cloud model parameters using a theoretical backscatter model. *International Journal of Remote Sensing*, **23** (23): 5129—5133
- Inoue Y, Kurosu T, Maeno H, Uratsuka S, Kozu T, Dabrowska Z K and Qi J. 2002. Season-long daily measurements of multifrequency (Ka, Ku, X, C, and L) and full-polarization backscatter signatures over paddy rice fields and their relationship with biological variables. *Remote Sensing of Environment*, **81**:194—204
- Koay J Y, Tan C P, Lim K S, Abu Bakar S B, bin Abu Bakar S B, Ewe H T, Chuan H T and Kong J A. 2007. Paddy fields as electrically dense media: Theoretical modeling and measurement comparisons. *IEEE Transactions on Geoscience and Remote Sensing*, **45**(9):2837—2849
- Kuan D T, Sawchuk A A, Strand T C and Chavel P. 1987. Adaptive restoration of image with speckle. *IEEE Transactions on Acoustics, Speech, and Signal Processing*, **35**(3):373—383
- Le Toan T, Ribbes F, Wang L F, Floury N, Ding K H, Kong J A, Fujita M and Kurosu T. 1997. Rice crop mapping and monitoring using ERS-1 data based on experiment and modeling results. *IEEE Transactions of Geoscience and Remote Sensing*, **35**(1):41—56
- Li Z J, Zhou Y and Hapuarachchi H A P. 2004. Application of global optimization to calibration of Xin'anjiang model. *Journal of Hohai University (Natural Sciences)*, **32**(4):376—379
- Ma Y P, Wang S L, Zhang L and Hou Y Y. 2005. A preliminary study on the re-initialization/re-parameterization of a crop model based on remote sensing data. *Acta Phytocologica Sinica*, **29**(6): 918—926
- Mattia F, Le Toan T, Picard G, Posa F I, D'Alessio A, Notarnicola C, Gatti A M, Rinaldi M, Satalino G and Pasquariello G. 2003. Multitemporal C-Band radar measurements on wheat fields. *IEEE Transactions on Geoscience and Remote Sensing*, **41**(7):1551—1560
- Moulin S, Bondeau A and Delecote R. 1998. Combining agricultural crop models and satellite observations: From field to regional scales. *International Journal of Remote Sensing*, **19** (6): 1021—1036
- Quegan S and Yu J J. 2001. Filtering of multichannel SAR images. *IEEE Transactions on Geoscience and Remote Sensing*, **39**(11): 2372—2379
- Shao Y, Fan X T, Liu H, Xiao J, Ross S, Brisco B, Brown R and Staples G. 2001. Rice monitoring and production estimation using multi-temporal RADARSAT. *Remote Sensing of Environment*, **76**: 310—325
- Stankiewicz K A. 2006. The efficiency of crop recognition on ENVISAT ASAR images in two growing seasons. *IEEE Transactions on Geoscience and Remote Sensing*, **44**(4):806—814
- Tan B X, Li Z Y, Li B B and Zhang P P. 2006. Rice field mapping and monitoring using single-temporal and dual polarized ENVISAT ASAR data. *Transactions of the CSAE*, **22**(12):121—127
- Wigneron J P, Ferrazzoli P, Olioso A, Bertuzzi P and Chanzy A. 1999. A simple approach to monitor crop biomass from C-Band radar data. *Remote Sensing of Environment*, **69**:179—188
- Xue C Y, Yang X G, Bouman B A M, Fen L P, van Laar G, Wang H Q, Wang P and Wang Z M. 2005. Preliminary approach on adaptability of ORYZA2000 model for aerobic rice in Beijing region. *ACTA AGRONOMICA SINICA*, **31**(12):1567—1571
- Yan Y, Liu Q H, Liu Q, Li J and Chen L F. 2006. Methodology of winter wheat yield prediction based on assimilation of remote sensing data with crop growth model. *Journal of Remote Sensing*, **10**(5):804—811
- Yang S B, Li B B, Shen S H and Zhang P P. 2006. Structure retaining linear multi-channel SAR image speckle filter. *ACTA GEODAEITICA et CARTOGRAPHICA SINICA*, **35**(11):364—370
- Yang S B, Shen S H, Li B B, Le Toan T and He W. 2008a. Rice mapping and monitoring using ENVISAT ASAR data. *IEEE Geoscience and Remote Sensing Letters*, **5**(1):108—112
- Yang S B, Li B B, Shen S H, Tan B X and He W. 2008b. Rice mapping research based on multi-temporal, multi-polarization backscattering differences. *Journal of Remote Sensing*, **12**(3):138—144
- Yu H L, Shen Y Q, Li W X, *et al.* 1980. Crop cultivation science (Volume One). Beijing: Agricultural Publishing House
- Zhang P P, Shen S H and Li B B. 2006. Study on rice polarization backscatter signatures and rice mapping methodology. *Jiangsu Agricultural Sciences*, (1):148—152
- Zhao Y X, Zhou X J and Liang S L. 2005. Methods and application of coupling remote sensing data and crop growth models: Advance in research. *Journal of Natural Disasters*, **14**(1):103—109



# ASAR 数据与水稻作物模型同化

## 制作水稻产量分布图

杨沈斌<sup>1</sup>, 申双和<sup>1</sup>, 李秉柏<sup>2</sup>, 谭炳香<sup>3</sup>, 李增元<sup>3</sup>

- 1. 南京信息工程大学 应用气象学院, 江苏 南京 210044;
- 2. 江苏省农业科学院 农业资源与环境研究所, 江苏 南京 210014;
- 3. 中国林业科学院 资源信息研究所, 北京 100091

**摘 要:** 提出了利用雷达数据进行水稻估产的技术方法,并以 ASAR 数据为例,探讨了雷达数据在水稻估产中的可行性。首先利用 ASAR 数据进行水稻制图,从各时相 ASAR 数据中提取水稻后向散射系数。随后,基于像元尺度,采用同化方法,以 LAI 为结合点,将水稻作物模型 ORYZA2000 与半经验水稻后向散射模型结合,建立嵌套模型模拟水稻后向散射系数。选择水稻出苗期和播种密度为参数优化对象,利用全局优化算法 SCE-UA 对 ORYZA2000 模型重新初始化,使模拟的水稻后向散射系数值与实测值误差最小,并由优化后的 ORYZA2000 模型计算每个像元的水稻产量,生成水稻产量分布图。结果表明,水稻产量分布图能够描绘研究区水稻实际产量的分布趋势,但由于采用潜在生长条件模拟,模拟的水稻平均产量比实测平均值高约 13%,验证点的水稻产量模拟值与实测值相对误差为 11.2%。由于半经验水稻后向散射模型存在对 LAI 变化不够敏感和对水层的简化处理,增加了水稻估产的误差。但从总体上看,利用该方法进行区域水稻估产是可行的,并为多云多雨地区的水稻遥感监测提供了重要参考。

**关键词:** 同化方法,遥感,ASAR,水稻估产,作物模型